

3D correlation imaging for localized phase disturbance mitigation

Francesco V. Pepe^{1,2} and Milena D'Angelo^{1,2}

¹*Dipartimento di Fisica, Università di Bari, I-70126 Bari, Italy*

²*INFN, Sezione di Bari, I-70125 Bari, Italy*

Correlation plenoptic imaging is a procedure to perform light-field imaging without spatial resolution loss, by measuring second-order spatio-temporal correlations of light. We investigate the possibility to use correlation plenoptic imaging to mitigate the effect of a phase disturbance in the propagation from the object to the main lens. We assume that this detrimental effect, that can be due to a turbulent medium, is localized at a specific distance from the lens, and is slowly varying in time. The mitigation of turbulence effects has already fostered the development of both light-field imaging and correlation imaging procedures. Here, we aim at merging these aspects, proposing a correlation light-field imaging method to overcome the effects of slowly varying turbulence, without the loss of lateral resolution, typical of traditional plenoptic imaging devices.

I. INTRODUCTION

The class of plenoptic (or light-field) imaging methods includes protocols and devices that are aimed to detect the *light field*, namely the joint information, within the limits of wave optics, on the light spatial distribution and propagation direction [1–5]. Interestingly, plenoptic imaging allows retrieving such a three-dimensional information retrieval in a single intensity acquisition, while making use of no interferometric measurements. This technique is currently used in diverse scientific and technical application fields, which include microscopy [6–9], stereoscopy [10–12], wavefront sensing [13–17], particle tracking and sizing [18], particle image velocimetry [19], and 3D neuronal activity functional imaging [9, 20]. Through the acquired directional information, plenoptic devices open the possibility to perform viewpoint changes, refocusing at different axial distances and, consequently, three dimensional reconstruction of the a finite volume [21]. In state-of-art-devices, the key to achieve plenoptic imaging is to combine the main lens with an array of micro-lenses [2, 22], which encode on the detector a composite information on the light-field. However, in all the implementations based on first-order intensity measurement, the drawback of such a structure is a limitation of the lateral resolution, that becomes inversely proportional to the gain in directional resolution, making the Rayleigh limit set by the numerical aperture of the main lens unreachable.

In the context of intensity correlation imaging [23–31], a way to overcome this practical limitation emerged in a technique named correlation plenoptic imaging (CPI), capable of performing plenoptic imaging without spatial resolution loss by measuring second-order spatio-temporal correlations of light [32, 33]. Thanks to the correlation between light beams of either chaotic light or entangled photons [32, 34–41], such a measurement encodes information not only on the spatial distribution of light in a given plane in the scene, but also on the direction of light. This method entails a relevant qualitative and quantitative mitigation of the trade-off between spatial and directional resolution, opening the way to a dramatic performance increase in terms of volumetric resolution, which is especially relevant when correlation measurements are performed through high-speed spatially resolving detectors [41, 42].

In this article, we investigate the possibility to exploit CPI to mitigate the effect of a phase disturbance in the propagation from the object to the main lens. We assume that this detrimental effect, that can be due to a turbulent medium, is localized at a specific distance from the lens, and is slowly varying in time. The presence of turbulence is an outstanding challenge of imaging, that fosters the research for new tools and devices [43]. Interestingly, one of these attempts at mitigating turbulence involves standard light-field imaging, in view of its possibility to detect the direction of light coming from specific points of the scene [44, 45]. On the other hand, much research has been devoted to determining the robustness to turbulence of correlation imaging methods [46–52]. Our aim here is to merge these aspect, proposing a correlation light-field imaging method to overcome the effects of slowly varying turbulence, without the loss of lateral resolution, typical of traditional plenoptic imaging devices.

The article is organized as follows. In Section 2, we show the detrimental effect of an axially localized phase disturbance on the first-order image collected by a standard imaging device. In Section 3, we discuss how to exploit correlation imaging to obtain a collection of sharp images of an object by CPI, despite the presence of the considered turbulence. In Section 4, we comment on how to maximize the information extraction from the CPI measurements, and how the technique can be integrated with innovative sensors and data analysis protocols.

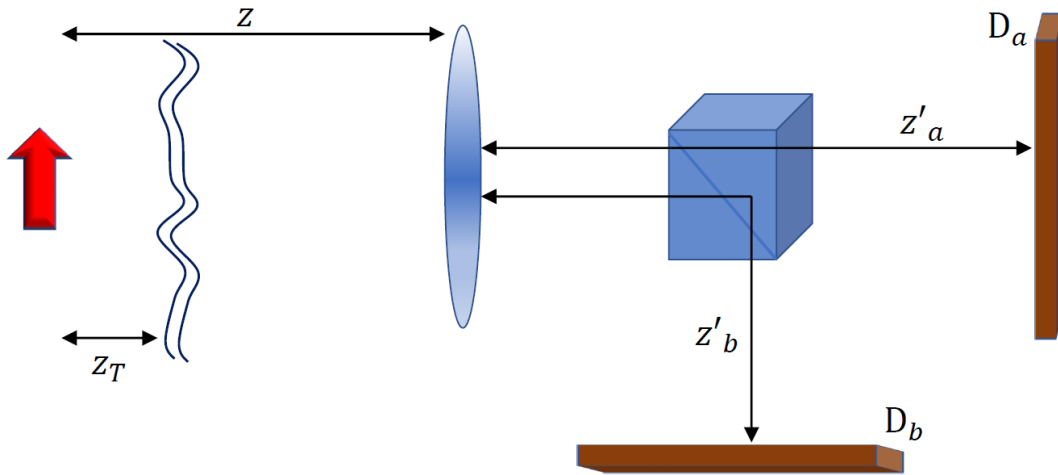


FIG. 1. Optical scheme of the setup described in the article. Light from an object, treated as a chaotic emitter, encounters turbulence in a thin region of space, at a distance z_T , before impinging on the lens. After the lens, light is split in two optical paths, impinging on the spatially-resolving sensors D_a and D_b , respectively. The lens-to-sensor distances z'_j , with $j = a, b$, define two object planes at the respective conjugate distances z_j , satisfying $1/z_j + 1/z'_j = 1/f$, with f the focal length of the lens. The signal is collected by measuring pixel-by-pixel correlations between intensity fluctuations on the two sensors.

II. FIRST-ORDER IMAGING WITH AN AXIALLY LOCALIZED TURBULENCE

The optical scheme that we considered in this article, shown in Fig. 1, is based on the paradigm of correlation plenoptic imaging between arbitrary planes (CPI-AP) [37]. It consists in a single lens of focal length f , that collects chaotic light emitted by the object, placed at an arbitrary distance z , which undergoes turbulence at a distance z_T on its way to the lens. After the lens, light is split in two paths by a beam splitter. The two beams impinge on the sensors D_a and D_b , placed at distances z'_a and z'_b , respectively. These two distances define two object planes at distances z_a and z_b in front of the lens, through the equations

$$\frac{1}{z_j} + \frac{1}{z'_j} = \frac{1}{f}, \quad \text{with } j = a, b. \quad (1)$$

The results here presented are based on the following assumptions on turbulence:

- Turbulence occurs upstream of the beam splitter, i.e. in the region where the optical paths are superposed.
- Turbulence is slowly varying in time, and can be approximated as quasi-static in the time required to perform a reasonable reconstruction of the correlation function.
- Turbulence is due to unpredictable perturbations of the refractive index in a region of space of small longitudinal extension Δz , such that its effect amounts to multiplying the field in that region by a phase factor $\exp(ik\Delta n(\boldsymbol{\rho}_T)\Delta z)$, with $\boldsymbol{\rho}_T$ the transverse coordinate of the turbulence plane and $\Delta n(\boldsymbol{\rho}_T)$ the change in refractive index with respect to the background. Notice, instead, that turbulence in a thick region should be described by a convolution of the field [53].

To explain the detrimental effect of turbulence, it is instructive to start from the first-order results, namely the intensity measured at the end of one of the optical paths. Neglecting, for the sake of simplicity, the finite aperture of the lens, the field propagator from an object point of coordinate $\boldsymbol{\rho}_o$ and a point of coordinate $\boldsymbol{\rho}_a$ on the sensor D_j reads

$$g_j(\boldsymbol{\rho}_j, \boldsymbol{\rho}_o) = C_j e^{ik\psi(\boldsymbol{\rho}_j)} \exp\left(\frac{ik\rho_o^2}{2z_T}\right) \times \int d^2\boldsymbol{\rho}_T \exp\left\{ik\left[\left(\frac{1}{z_T} - \frac{1}{z_T + z_j - z}\right)\frac{\boldsymbol{\rho}_T^2}{2} - \frac{\boldsymbol{\rho}_T}{z_T} \cdot \left(\boldsymbol{\rho}_o + \frac{z_T}{z_T + z_j - z} \frac{\boldsymbol{\rho}_j}{M_j}\right) - \phi(\boldsymbol{\rho}_T)\right]\right\}, \quad (2)$$

where $\phi(\boldsymbol{\rho}_T) = \Delta n(\boldsymbol{\rho}_T)\Delta z$ determines the phase change due to turbulence, and $M_j = z'_j/z_j$, with $j = a, b$, are the absolute magnifications of the images focused by the lens on the two sensors. If the object is a chaotic-light emitter with intensity profile $\mathcal{A}(\boldsymbol{\rho}_o)$, the intensity measured on each sensor D_j reads

$$I_j(\boldsymbol{\rho}_j) = \int d^2\boldsymbol{\rho}_o \mathcal{A}(\boldsymbol{\rho}_o) |g_j(\boldsymbol{\rho}_j, \boldsymbol{\rho}_o)|^2. \quad (3)$$

In the case in which we are most interested, when the object is focused on D_j (namely, $z = z_j$), the intensity reads, up to irrelevant constants,

$$I_j(\boldsymbol{\rho}_j) = \int d^2\boldsymbol{\rho}_o \mathcal{A}(\boldsymbol{\rho}_o) \left| \int d^2\boldsymbol{\rho}_T \exp \left\{ ik \left[\phi(\boldsymbol{\rho}_T) - \frac{1}{z_T} \boldsymbol{\rho}_T \cdot \left(\boldsymbol{\rho}_o + \frac{\boldsymbol{\rho}_j}{M_j} \right) \right] \right\} \right|^2, \quad (4)$$

leading to the stigmatic image $\mathcal{A}(-\boldsymbol{\rho}_j/M_j)$, inverted and magnified by M_j , in the case of no turbulence. When turbulence is present, we can characterize its effect by considering the limit of geometrical optics $k \rightarrow \infty$, and the stationary-phase approximation [54], leading to

$$I_j(\boldsymbol{\rho}_j) \sim \int d^2\boldsymbol{\rho}_T \mathcal{A} \left(-\frac{\boldsymbol{\rho}_j}{M_j} + z_T \nabla \phi(\boldsymbol{\rho}_T) \right). \quad (5)$$

Therefore, in the presence of turbulence, rays passing from a point $\boldsymbol{\rho}_T$ on the turbulence plane are deviated by an amount proportional to the gradient of the phase disturbance ϕ , leading to the superposition of sub-images characterized by different shifts. This situation closely resembles the case of an out-of-focus object, which is commonly tackled by plenoptic imaging, with the relevant difference that, in the case of turbulence, the image shift is unpredictable a priori. Notice that the effect of turbulence is less and less relevant as it occurs closer to the sample ($z_T \rightarrow 0$), as the spread due to turbulence at some point becomes less important than the natural point-spread due to the finite lens aperture.

III. CPI FOR TURBULENCE MITIGATION

Intuitively, as it occurs in CPI to reconstruct out-of-focus images, if correlation measurement is able to detect each single sub-image with a well-defined shift, the detrimental effect of the superposition of shifted images in Eq. (5) can be avoided. Therefore, let us consider the correlation function $\Gamma(\boldsymbol{\rho}_a, \boldsymbol{\rho}_b)$ between intensity fluctuations in the couple of points $\boldsymbol{\rho}_a$ on the sensor D_a and $\boldsymbol{\rho}_b$ on D_b . Treating the object as a chaotic light emitter, as in Eq. (3), one obtains

$$\Gamma(\boldsymbol{\rho}_a, \boldsymbol{\rho}_b) = \left| \int d^2\boldsymbol{\rho}_o \mathcal{A}(\boldsymbol{\rho}_o) g_a(\boldsymbol{\rho}_a, \boldsymbol{\rho}_o) g_b^*(\boldsymbol{\rho}_b, \boldsymbol{\rho}_o) \right|^2. \quad (6)$$

Before treating the plenoptic-based reconstruction of the image, it is worth observing that the autocorrelation of intensity fluctuations

$$\Gamma(\boldsymbol{\rho}_a, \boldsymbol{\rho}_b) = I_a^2(\boldsymbol{\rho}_a) \quad (7)$$

coincides with the squared first-order intensity. This result could entail an apparent mitigation of turbulence in second-order measurement. However, the average result of autocorrelation measurement is indistinguishable from measuring intensity and squaring the result; therefore, an effective mitigation occurs only if noise affecting $\Gamma(\boldsymbol{\rho}_a, \boldsymbol{\rho}_b)$ is lower than the one affecting $I_a^2(\boldsymbol{\rho}_a)$. This will be the object of further analysis.

Going back to the general form of Γ , the result for the setup in Fig. 1 can be evaluated by inserting the propagators (2), yielding, up to irrelevant constants,

$$\Gamma(\boldsymbol{\rho}_a, \boldsymbol{\rho}_b) = \left| \int d^2\boldsymbol{\rho}_o \int d^2\boldsymbol{\rho}_T \int d^2\boldsymbol{\rho}'_T \mathcal{A}(\boldsymbol{\rho}_o) \exp [ik\Psi(\boldsymbol{\rho}_a, \boldsymbol{\rho}_b; \boldsymbol{\rho}_o, \boldsymbol{\rho}_T, \boldsymbol{\rho}'_T)] \right|^2, \quad (8)$$

where

$$\begin{aligned} \Psi(\boldsymbol{\rho}_a, \boldsymbol{\rho}_b; \boldsymbol{\rho}_o, \boldsymbol{\rho}_T, \boldsymbol{\rho}'_T) = & \left(\frac{1}{z_T} - \frac{1}{z_T + z_a - z} \right) \frac{\boldsymbol{\rho}_T^2}{2} - \left(\frac{1}{z_T} - \frac{1}{z_T + z_b - z} \right) \frac{\boldsymbol{\rho}'_T{}^2}{2} \\ & - \frac{1}{z_T} \boldsymbol{\rho}_o \cdot (\boldsymbol{\rho}_T - \boldsymbol{\rho}'_T) - \frac{1}{z_T + z_a - z} \boldsymbol{\rho}_T \cdot \frac{\boldsymbol{\rho}_a}{M_a} + \frac{1}{z_T + z_b - z} \boldsymbol{\rho}'_T \cdot \frac{\boldsymbol{\rho}_b}{M_b} + \phi(\boldsymbol{\rho}_T) - \phi(\boldsymbol{\rho}'_T). \end{aligned} \quad (9)$$

The stationary-phase conditions

$$\nabla_{\rho_0} \Psi = \nabla_{\rho_T} \Psi = \nabla_{\rho'_T} \Psi = 0, \quad (10)$$

that determine the point(s) $(\bar{\rho}_o, \bar{\rho}_T, \bar{\rho}'_T)$ providing dominant contribution in the geometrical-optics limit $k \rightarrow \infty$, do not form a linear system in the integration variables, as it would occur in absence of turbulence, due to the presence of $\nabla\phi$. However, the system is solvable anyway, as the equation that determines the stationary values of ρ_T and ρ'_T is linear and independent of both ρ_o and the phase variation gradient, leading to the solution

$$\bar{\rho}_T = \bar{\rho}'_T = \frac{1}{z_a - z_b} \left[(z_T + z_b - z) \frac{\rho_a}{M_a} - (z_T + z_a - z) \frac{\rho_b}{M_b} \right]. \quad (11)$$

This enables to determine the stationary value of ρ_o through the remaining independent condition, leading to

$$\bar{\rho}_o = -\frac{1}{z_a - z_b} \left[(z - z_b) \frac{\rho_a}{M_a} + (z_a - z) \frac{\rho_b}{M_b} \right] + z_T \nabla\phi(\bar{\rho}_T). \quad (12)$$

Therefore, despite the turbulence, the dominant contribution to the correlation function comes from a single object point,

$$\Gamma(\rho_a, \rho_b) \sim \mathcal{A}^2 \left(-\frac{1}{z_a - z_b} \left[(z - z_b) \frac{\rho_a}{M_a} + (z_a - z) \frac{\rho_b}{M_b} \right] + z_T \nabla\phi \left(\frac{1}{z_a - z_b} \left[(z_T + z_b - z) \frac{\rho_a}{M_a} - (z_T + z_a - z) \frac{\rho_b}{M_b} \right] \right) \right), \quad (13)$$

providing a *single* shifted image for each pair of points (ρ_a, ρ_b) . Clearly, this image is detectable only provided the time scale of turbulence is slow enough to permit the reconstruction of the correlation function with a reasonable signal-to-noise ratio. Specializing the result to the case of reference, in which the object is focused on D_a (for definiteness), with $z = z_a$, the correlation function takes the interesting form

$$\Gamma(\rho_a, \rho_b) \sim \mathcal{A}^2 \left(-\frac{\rho_a}{M_a} + z_T \nabla\phi \left(\frac{1}{z_a - z_b} \left[(z_T + z_b - z_a) \frac{\rho_a}{M_a} - z_T \frac{\rho_b}{M_b} \right] \right) \right), \quad (14)$$

the parallel with Eq. (5) becomes clear: the choice of (ρ_a, ρ_b) addresses a particular point on the turbulence plane, and therefore a specific shift of the image. Notice that the dependence of Γ on ρ_b can be used as an indicator to detect the presence of turbulence with a transverse gradient. The situation when the turbulence plane is focused on D_b , namely $z_b = z_a - z_T$,

$$\Gamma(\rho_a, \rho_b) \sim \mathcal{A}^2 \left(-\frac{\rho_a}{M_a} + z_T \nabla\phi \left(-z_T \frac{\rho_b}{M_b} \right) \right), \quad (15)$$

becomes even simpler (and intuitive). Once the different sub-images, obtained by evaluating with varying ρ_b , are collected, one can evaluate their relative alignment (e.g. by computing the point-to-point correlation between them) and follow two strategies to obtain an integrated image with higher signal-to-noise ratio:

- sum only those sub-images characterized by the dominant alignment;
- realign all the sub-images and sum over them.

It is worth remarking that, due to the plenoptic properties of the correlation function, the advantage is not limited to the case of a focused object. However, though one can in principle reconstruct images of objects placed out of focus, wave-optics computation shows that the resolution of the correlation images is maximal in focus [33]. Here, resolution is determined by the Rayleigh limit, that is unattainable by traditional light-field techniques [33, 39, 40, 55, 56].

IV. DISCUSSION AND OUTLOOK

The results outlined in the previous section show that the light-field capability of CPI can be used to trace back the image of an object through phase disturbance, by using intensity correlations to isolate the contribution of a limited

area of the turbulence plane. Compared to analogous applications of standard light-field imaging to turbulence mitigation [44, 45], CPI potentially provides at the same time diffraction-limited resolution on the focused plane, and a much wider variety of independent viewpoints on a 3D sample [32]. Even though our analysis is limited to a focused object and to the geometrical-optics regime, recent wave-optics results demonstrated that the out-of-focus imaging properties of CPI entail a better volumetric resolution than any non-scanning first-order method [57].

One of the possible limitations of the method is related to the intrinsic need of CPI for collecting a large number of frames, to provide a stable statistical reconstruction of the correlation function. If the phase disturbance is not constant, the acquisition time must not exceed the typical variation time of the perturbation, to prevent different phase gradients from contributing to the same correlation evaluation [see Eqs. (14)-(15)]. Keeping the acquisition time short, in turn, can lead to noisy images. Therefore, the technique can largely benefit from new sensors that combine high-resolution with low noise and gating times close to the nanosecond [42, 58–60], already applied to a CPI-AP experiment in a non-turbulent environment [41]. Moreover, further potential development can come from integrating the described methods with tools to maximize information extraction from data, like compressive sensing [61] and artificial intelligence [62], which can specifically help to realign noisy sub-images, even taken at different times.

Future research will be devoted to the analysis of phase disturbance effects on different methods of plenoptic imaging with intensity correlations, such as light-field ghost imaging [63]), and to generalizing the results to different models of turbulence.

-
- [1] E. H. Adelson and J. Y. Wang, Single lens stereo with a plenoptic camera, *IEEE transactions on pattern analysis and machine intelligence* **14**, 99 (1992).
 - [2] R. Ng, M. Levoy, M. Brédif, G. Duval, M. Horowitz, and P. Hanrahan, Light field photography with a hand-held plenoptic camera, *Computer Science Technical Report CSTR* **2**, 1 (2005).
 - [3] R. Ng, Fourier slice photography, *ACM Transactions on Graphics* **24**, 735 (2005).
 - [4] G. Wu, B. Masia, A. Jarabo, Y. Zhang, L. Wang, Q. Dai, T. Chai, and Y. Liu, Light Field Image Processing: An Overview, *IEEE J. Sel. Top. Signal Process.* **11**, 926 (2017).
 - [5] E. Y. Lam, Computational photography with plenoptic camera and light field capture: tutorial, *J. Opt. Soc. Am. A* **32**, 2021 (2015).
 - [6] M. Levoy, R. Ng, A. Adams, M. Footer, and M. Horowitz, Light field microscopy, *ACM Transactions on Graphics (TOG)* **25**, 924 (2006).
 - [7] M. Broxton, L. Grosenick, S. Yang, N. Cohen, A. Andalman, K. Deisseroth, and M. Levoy, Wave optics theory and 3-d deconvolution for the light field microscope, *Optics express* **21**, 25418 (2013).
 - [8] W. Glastre, O. Hugon, O. Jacquin, H. G. de Chatellus, and E. Lacot, Demonstration of a plenoptic microscope based on laser optical feedback imaging, *Optics Express* **21**, 7294 (2013).
 - [9] R. Prevedel, Y.-G. Yoon, M. Hoffmann, N. Pak, G. Wetzstein, S. Kato, T. Schrödel, R. Raskar, M. Zimmer, E. S. Boyden, *et al.*, Simultaneous whole-animal 3d imaging of neuronal activity using light-field microscopy, *Nature Methods* **11**, 727 (2014).
 - [10] E. H. Adelson and J. Y. Wang, Single lens stereo with a plenoptic camera, *IEEE transactions on pattern analysis and machine intelligence* **14**, 99 (1992).
 - [11] S. Muenzel and J. W. Fleischer, Enhancing layered 3d displays with a lens, *Applied Optics* **52**, D97 (2013).
 - [12] M. Levoy and P. Hanrahan, Light field rendering, in *Proceedings of the 23rd annual conference on Computer graphics and interactive techniques* (ACM, 1996) pp. 31–42.
 - [13] C. Wu, *The plenoptic sensor*, Ph.D. thesis, University of Maryland, College Park (2016).
 - [14] Y. Lv, R. Wang, H. Ma, X. Zhang, Y. Ning, and X. Xu, Su-g-iep4-09: Method of human eye aberration measurement using plenoptic camera over large field of view, *Medical Physics* **43**, 3679 (2016).
 - [15] C. Wu, J. Ko, and C. C. Davis, Using a plenoptic sensor to reconstruct vortex phase structures, *Optics Letters* **41**, 3169 (2016).
 - [16] C. Wu, J. Ko, and C. C. Davis, Imaging through strong turbulence with a light field approach, *Optics Express* **24**, 11975 (2016).
 - [17] J. Ko and C. C. Davis, Comparison of the plenoptic sensor and the shack–hartmann sensor, *Applied Optics* **56**, 3689 (2017).
 - [18] E. M. Hall, B. S. Thurrow, and D. R. Guildenbecher, Comparison of three-dimensional particle tracking and sizing using plenoptic imaging and digital in-line holography, *Applied Optics* **55**, 6410 (2016).
 - [19] T. W. Fahringer, K. P. Lynch, and B. S. Thurrow, Volumetric particle image velocimetry with a single plenoptic camera, *Measurement Science and Technology* **26**, 115201 (2015).
 - [20] O. Skocek, T. Noebauer, L. Weilguny, F. Martínez Traub, C. Xia, M. Molodtsov, A. Grama, M. Yamagata, D. Aharoni, D. Cox, P. Golshani, and A. Vaziri, High-speed volumetric imaging of neuronal activity in freely moving rodents, *Nat. Methods* **15**, 429 (2018).
 - [21] X. Xiao, B. Javidi, M. Martinez-Corral, and A. Stern, Advances in three-dimensional integral imaging: sensing, display, and applications [invited], *Applied Optics* **52**, 546 (2013).

- [22] T. G. Georgiev and A. Lumsdaine, Focused plenoptic camera and rendering, *Journal of Electronic Imaging* **19**, 021106 (2010).
- [23] T. B. Pittman, Y.-H. Shih, D. V. Strekalov, and A. V. Sergienko, Optical imaging by means of two-photon quantum entanglement, *Phys. Rev. A* **52**, R3429 (1995).
- [24] R. S. Bennink, S. J. Bentley, and R. W. Boyd, “Two-photon” coincidence imaging with a classical source, *Phys. Rev. Lett.* **89**, 113601 (2002).
- [25] A. Valencia, G. Scarcelli, M. D’Angelo, and Y. Shih, Two-photon imaging with thermal light, *Phys. Rev. Lett.* **94**, 063601 (2005).
- [26] A. Gatti, E. Brambilla, M. Bache, and L. A. Lugiato, Ghost imaging with thermal light: comparing entanglement and classical correlation, *Phys. Rev. Lett.* **93**, 093602 (2004).
- [27] G. Scarcelli, V. Berardi, and Y. Shih, Can two-photon correlation of chaotic light be considered as correlation of intensity fluctuations?, *Phys. Rev. Lett.* **96**, 063602 (2006).
- [28] M. N. O’Sullivan, K. W. C. Chan, and R. W. Boyd, Comparison of the signal-to-noise characteristics of quantum versus thermal ghost imaging, *Phys. Rev. A* **82**, 053803 (2010).
- [29] G. Brida, M. Chekhova, G. Fornaro, M. Genovese, E. Lopaeva, and I. R. Berchera, Systematic analysis of signal-to-noise ratio in bipartite ghost imaging with classical and quantum light, *Phys. Rev. A* **83**, 063807 (2011).
- [30] M. Cassano, M. D’Angelo, A. Garuccio, T. Peng, Y. Shih, and V. Tamma, Spatial interference between pairs of disjoint optical paths with a chaotic source, *Opt. Express* **25**, 6589 (2017).
- [31] M. D’Angelo, A. Mazzilli, F. V. Pepe, A. Garuccio, and V. Tamma, Characterization of two distant double-slits by chaotic light second-order interference, *Sci. Rep.* **7**, 2247 (2017).
- [32] M. D’Angelo, F. V. Pepe, A. Garuccio, and G. Scarcelli, Correlation plenoptic imaging, *Physical Review Letters* **116**, 223602 (2016).
- [33] F. V. Pepe, F. Di Lena, A. Mazzilli, E. Edrei, A. Garuccio, G. Scarcelli, and M. D’Angelo, Diffraction-limited plenoptic imaging with correlated light, *Physical Review Letters* **119**, 243602 (2017).
- [34] F. V. Pepe, G. Scarcelli, A. Garuccio, and M. D’Angelo, Plenoptic imaging with second-order correlations of light, *Quantum Measurements and Quantum Metrology* **3**, 20 (2016).
- [35] F. V. Pepe, F. Di Lena, A. Garuccio, G. Scarcelli, and M. D’Angelo, Correlation plenoptic imaging with entangled photons, *Technologies* **4**, 17 (2016).
- [36] F. V. Pepe, O. Vaccarelli, A. Garuccio, G. Scarcelli, and M. D’Angelo, Exploring plenoptic properties of correlation imaging with chaotic light, *Journal of Optics* **19**, 114001 (2017).
- [37] F. Di Lena, G. Massaro, A. Lupo, A. Garuccio, F. V. Pepe, and M. D’Angelo, Correlation plenoptic imaging between arbitrary planes, *Optics Express* **28**, 35857 (2020).
- [38] A. Scagliola, F. Di Lena, A. Garuccio, M. D’Angelo, and F. V. Pepe, Correlation plenoptic imaging for microscopy applications, *Phys. Lett. A* , 126472 (2020).
- [39] G. Massaro, F. Di Lena, M. D’Angelo, and F. V. Pepe, Effect of finite-sized optical components and pixels on light-field imaging through correlated light, *Sensors* **22**, 2778 (2022).
- [40] G. Massaro, F. V. Pepe, and M. D’Angelo, Refocusing Algorithm for Correlation Plenoptic Imaging, *Sensors* **22**, 6665 (2022).
- [41] G. Massaro, P. Mos, S. Vasiukov, F. Di Lena, F. Scattarella, F. V. Pepe, A. Ulku, D. Giannella, E. Charbon, C. Bruschini, and M. D’Angelo, Correlated-photon imaging at 10 volumetric images per second, *Sci. Rep.* **13**, 12813 (2023).
- [42] C. Abbattista, L. Amoruso, S. Burri, E. Charbon, F. Di Lena, A. Garuccio, D. Giannella, Z. Hradil, M. Iacobellis, G. Massaro, *et al.*, Towards quantum 3d imaging devices, *Applied Sciences* **11**, 6414 (2021).
- [43] C. R. Michael and M. W. Byron, *Imaging Through Turbulence* (CRC Press, Boca Raton, Florida, 1996).
- [44] C. Wu, J. Ko, and C. C. Davis, Imaging Through Turbulence Using a Plenoptic Sensor, *Proc. SPIE* **9614**, 961405 (2015).
- [45] C. Wu, J. Ko, and C. C. Davis, Imaging through strong turbulence with a light field approach, *Optics express* **24**, 11975 (2016).
- [46] J. Cheng, Ghost imaging through turbulent atmosphere, *Opt. Express* **17**, 7916 (2009).
- [47] C. Li, T. Wang, J. Pu, W. Zhu, and R. Rao, Ghost imaging with partially coherent light radiation through turbulent atmosphere, *Appl. Phys. B* **99**, 599 (2010).
- [48] K. W. C. Chan, D. S. Simon, A. V. Sergienko, N. D. Hardy, J. H. Shapiro, P. B. Dixon, G. A. Howland, J. C. Howell, J. H. Eberly, M. O’Sullivan, B. Rodenburg, and R. W. Boyd, Theoretical analysis of quantum ghost imaging through turbulence, *Phys. Rev. A* **84**, 043807 (2011).
- [49] N. D. Hardy and J. H. Shapiro, Reflective ghost imaging through turbulence, *Phys. Rev. A* **84**, 063824 (2011).
- [50] P. B. Dixon, G. A. Howland, K. W. C. Chan, C. O’Sullivan-Hale, B. Rodenburg, N. D. Hardy, J. H. Shapiro, D. S. Simon, A. V. Sergienko, R. W. Boyd, and J. C. Howell, Quantum ghost imaging through turbulence, *Phys. Rev. A* **83**, 051803 (2011).
- [51] R. E. Meyers, K. S. Deacon, and Y. Shih, Turbulence-free ghost imaging, *Applied Physics Letters* **98**, 111115 (2011).
- [52] D. Shi, C. Fan, P. Zhang, J. Zhang, H. Shen, C. Qiao, and Y. Wang, Adaptive optical ghost imaging through atmospheric turbulence, *Opt. Express* **20**, 27992 (2012).
- [53] R. L. Fante, Wave propagation in random media: a systems approach, in *Progress in Optics XXII*, edited by E. Wolf (Elsevier, Amsterdam, 1985).
- [54] B. E. A. Saleh and M. C. Teich, *Fundamentals of photonics* (John Wiley & Sons, New York, NY, 2007).
- [55] F. Scattarella, M. D’Angelo, and F. V. Pepe, Resolution limit of correlation plenoptic imaging between arbitrary planes, *Optics* **3**, 138 (2022).

- [56] F. Scattarella, G. Massaro, B. Stoklasa, M. D'Angelo, and F. V. Pepe, Periodic patterns for resolution limit characterization of correlation plenoptic imaging, *Eur. Phys. J. Plus* **138**, 710 (2023).
- [57] G. Massaro, D. Giannella, A. Scagliola, F. Di Lena, G. Scarcelli, A. Garuccio, F. V. Pepe, and M. D'Angelo, Light-field microscopy with correlated beams for extended volumetric imaging at the diffraction limit, *Sci. Rep.* **12**, 16823 (2022).
- [58] I. M. Antolovic, S. Burri, R. A. Hoebe, Y. Maruyama, C. Bruschini, and E. Charbon, Photon-counting arrays for time-resolved imaging, *Sensors* **16**, 1005 (2016).
- [59] G. Lubin, R. Tenne, I. M. Antolovic, E. Charbon, C. Bruschini, and D. Oron, Quantum correlation measurement with single photon avalanche diode arrays, *Opt. Express* **27**, 32863 (2019).
- [60] A. C. Ulku, A. Ardelean, I. M. Antolovic, S. Weiss, E. Charbon, C. Bruschini, and X. Michalet, Wide-field time-gated SPAD imager for phasor-based FLIM applications, *Methods Appl. Fluoresc.* **98**, 024002 (2020).
- [61] I. Petrelli, F. Santoro, G. Massaro, F. Scattarella, F. V. Pepe, F. Mazzia, M. Ieronymaki, G. Filios, D. Mylonas, N. Pappas, C. Abbattista, and M. D'Angelo, Compressive sensing-based correlation plenoptic imaging, *Front. Phys.* **11**, 1287740 (2023).
- [62] F. Scattarella, D. Diacono, A. Monaco, N. Amoroso, L. Bellantuono, G. Massaro, F. V. Pepe, S. Tangaro, R. Bellotti, and M. D'Angelo, Deep learning approach for denoising low-snr correlation plenoptic images, *Sci. Rep.* **13**, 19645 (2023).
- [63] A. Paniate, G. Massaro, A. Avella, A. Meda, F. V. Pepe, M. Genovese, M. D'Angelo, and I. Ruo-Berchera, Light-field ghost imaging, *Phys. Rev. Applied* **21**, 024032 (2024).